[redacted]

NACA RM L53B18

NACA

RESEARCH MEMORANDUM

A METHOD FOR CALCULATING THE AERODYNAMIC LOADING ON WING-TIP-TANK COMBINATIONS IN SUBSONIC FLOW

By Samuel W. Robinson, Jr., and Martin Zlotnick

Langley Aeronautical Laboratory
Langley Field, Va.

NATIONAL ADVISORY COMMITTEE
FOR AERONAUTICS

WASHINGTON

April 7, 1953

[redacted]

NACA RM L53B18

NATIONAL ADVISORY COMMITTEE FOR AERONAUTICS

RESEARCH MEMORANDUM

A METHOD FOR CALCULATING THE AERODYNAMIC LOADING ON WING–TIP-TANK COMBINATIONS IN SUBSONIC FLOW

By Samuel W. Robinson, Jr., and Martin Zlotnick

SUMMARY

An analytical method for calculating the aerodynamic loading on wing–tip-tank combinations in subsonic flow is developed by using a simple horseshoe vortex-image system for the case of the tank axis in the plane of the wing.

An illustrative example is given in the appendix, in which wing and tip-tank loadings are calculated for three configurations. The calculated results are shown to be in good agreement with experimental data.

INTRODUCTION

With external wing tip tanks coming into more general usage, an analytical method for calculating the effects of mutual interference between wing and tip tank will be valuable. This interference may cause large differences in wing torsion and bending moment from the wing-alone values and may introduce significant changes in the performance and stability characteristics of the aircraft.

Reference 1 presents a method for calculating the lift induced on the fuselage of a wing-fuselage combination for incompressible flow using as a basis for its development the mathematical model consisting of a set of horseshoe vortices and their images to represent a wing of arbitrary plan form in the presence of an infinite cylinder. This method affords a means of determining the distribution of the induced lift on the body and of the additional wing lift and is valid for configurations of varying plan forms and wing-span–body-diameter ratios. In using this method to compute loadings at high subsonic speeds, the

Prandtl-Glauert correction for compressibility may be applied in the same manner as for a wing alone.

In this paper, an extension of the work of reference 1 to the unsymmetrical case is made to provide a method of calculating the desired loadings on the wing–tip-tank combinations in which the tank axis lies in the plane of the wing.

SYMBOLS

A	aspect ratio, b^2/S
a	radius of an infinite circular cylinder representing the tip tank
b	wing span
C_L	lift coefficient, L/qS
C_{L_t}	tank lift coefficient, L_t/qS
C_{M_t}	tank pitching-moment coefficient, M/qSd_{max}
c_l	section lift coefficient, l/qc
c	wing chord
d	diameter of tip tank
e	length of tip tank
F,f	downwash functions for trailing vortex
G,g	downwash functions for bound vortex
l	section lift
L	total lift
M	total pitching moment
p	local pressure
q	free-stream dynamic pressure

[redacted]

r_t	radius of tip tank
s	semispan of reference horseshoe vortex, b/16
S	wing area
U	longitudinal component of free-stream velocity
u	longitudinal component of local velocity
V	volume
w	vertical component of local velocity (downwash)
x,y,z	longitudinal, lateral, and vertical coordinates, respectively
$\bar{x}$	longitudinal ordinate of center of pressure on tank
$\Delta y^{(i)}$	width of an image vortex
α	angle of attack
Γ	vortex strength
σ	correction factor for finite body length
η	correction factor for semi-infinite body
λ	taper ratio
Λ	sweep angle

Superscripts:

*	dimensionless with respect to b/2
'	dimensionless with respect to s
''	dimensionless with respect to r_t
'''	dimensionless with respect to d_{max}
(i)	function of image vortex

[redacted]

Subscripts:

n	running index, lift points or horseshoe vortices
m	number of horseshoe vortices representing wing
ot	center line of tip tank
p	index of downwash stations
g	geometric
t	pertaining to tip tank
w	pertaining to wing
wo	pertaining to wing alone
LE	leading edge of wing tip
T	pertaining to wing tip
u	upper surface of body
l	lower surface of body
wt	pertaining to wing–tip-tank combination
B	pertaining to body-alone component
$( )_\alpha$	slope per radian, $d/d\alpha$

BASIC CONSIDERATIONS

For analytical treatment, the wing–tip-tank combination in subsonic flow may be represented by a horseshoe vortex system similar to that used in reference 1 for wing-fuselage combinations. The wing is replaced by a set of horseshoe vortices and the tip tank, represented by an infinite cylinder, is replaced by the images of the wing vortices.

A mathematically rigorous solution to this idealized problem would require calculation of an additional potential within the cylinder, since the image vortices alone satisfy the boundary conditions only in particular locations on the cylinder. However, as in reference 1, this additional potential can be shown to produce zero net lift and moment on the cylinder. Therefore, using only the vortex-image system, a

[redacted]

straightforward method may be developed for calculating the lift induced on a cylindrical body attached to the wing tip. With modifications to the vortex-image system, the spanwise lift distribution on the wing with tank attached can be calculated approximately.

In addition to the induced lift component of the loading on the tip tank, which is independent of the angle of attack of the tip tank itself and which depends only on the spanwise loading of the wing, there is a relatively small component of loading due to the angle of attack of the body (referred to hereinafter as the "body alone" lift) which can be calculated approximately using Munk's airship theory. To treat a practical configuration, it is necessary to correct the induced lift on the tank slightly for finite body length, and the body-alone lift for the particular tank location.

The downwash behind the wing of a wing-tip-tank combination can also be calculated if desired by using the method of reference 1 as modified in this paper.

CALCULATION OF LIFT AND MOMENT ON TIP TANKS

In this section, the derivation of the expression for the induced lift on an infinite cylinder due to an external horseshoe vortex and its image within the cylinder is presented. The lift of each of a group of such vortices is superimposed to calculate the lift induced on a tip tank. This is followed by a calculation of the body-alone lift on a slender body of revolution, with corrections for the particular configuration. Added together, these two components give the total lift and moment on the tip tank.

Induced Lift

Vortex-image system.- A horseshoe vortex of width $y_2 - y_1$ outside of an infinite cylinder of radius a is shown in figure 1. An image horseshoe vortex of width $\frac{a^2}{y_1} - \frac{a^2}{y_2}$ lies within the cylinder, satisfying the boundary condition of zero flow normal to the cylinder wall only at $x = \pm\infty$, in the yz-plane at $x = 0$, and in the plane $z = 0$. Although in order to satisfy the boundary conditions everywhere else it would be necessary to superimpose an additional potential on the system, this additional potential has been shown in reference 1 to have zero net lift and pitching moment so that it need not be considered in this section.

Calculation of induced lift on a cylinder due to a vortex and its image.- The induced lift on a section dy of the cylinder in figure 1 is the integral of the pressure difference on the upper and lower surfaces of the section dy from $x = -\infty$ to $x = \infty$.

At two corresponding points on the upper and lower surfaces of the cylinder the local pressures are

$$p_u = \frac{1}{2}\rho(U + \Delta u_u)^2$$

$$p_l = \frac{1}{2}\rho(U + \Delta u_l)^2$$

The lift on the section dy is

$$\frac{dL}{dy} = \int_{-\infty}^{\infty} (p_u - p_l)\,dx \tag{1}$$

Now the vortex flow above the cylinder is equal and opposite to the flow at corresponding points below the cylinder; therefore,

$$\Delta u_u = -\Delta u_l$$

Expanding and simplifying the expressions for p_u and p_l yields

$$\frac{dL}{dy} = \int_{-\infty}^{\infty} 2\rho U\,\Delta u\,dx \tag{2}$$

The velocity induced on the cylinder surface by a vortex extending from y_1 to y_2 at (x,y,z), $V_{\Gamma_{y_1-y_2}}$ is given by the Biot-Savart law as

$$V_{\Gamma_{y_1-y_2}} = -\frac{\Gamma}{4\pi\sqrt{z^2 + x^2}}\left[\frac{y_1 - y}{\sqrt{z^2 + x^2 + (y_1 - y)^2}} - \frac{y_2 - y}{\sqrt{z^2 + x^2 + (y_2 - y)^2}}\right] \tag{3}$$

[redacted]

and for the image extending from a^2/y_1 to a^2/y_2

$$V_{\Gamma_{\frac{a^2}{y_1}-\frac{a^2}{y_2}}} = \frac{\Gamma}{4\pi\sqrt{z^2+x^2}}\left[\frac{\frac{a^2}{y_1}-y}{\sqrt{z^2+x^2+\left(\frac{a^2}{y_1}-y\right)^2}} - \frac{\frac{a^2}{y_2}-y}{\sqrt{z^2+x^2+\left(\frac{a^2}{y_2}-y\right)^2}}\right] \tag{4}$$

On the cylinder, Δu, the component of this flow parallel to the x-axis, is

$$\Delta u = V_\Gamma \cos\theta$$

where

$$\cos\theta = \frac{z}{\sqrt{z^2+x^2}}$$

Now, for the vortex-image system, the incremental velocity Δu is

$$\Delta u = -\frac{\Gamma z}{4\pi\left(z^2+x^2\right)}\left[\frac{y_1-y}{\sqrt{x^2+z^2+\left(y_1-y\right)^2}} - \frac{y_2-y}{\sqrt{x^2+z^2+\left(y_2-y\right)^2}} + \frac{\frac{a^2}{y_2}-y}{\sqrt{x^2+z^2+\left(y-\frac{a^2}{y_2}\right)^2}} - \frac{\frac{a^2}{y_1}-y}{\sqrt{x^2+z^2+\left(y-\frac{a^2}{y_1}\right)^2}}\right] \tag{5}$$

where, on the surface of the cylinder $z = \sqrt{a^2-y^2}$.

[redacted]

Since

$$\frac{dL}{dy} = \int_{-\infty}^{\infty} 2\rho U \, \Delta u \, dx \tag{6}$$

substitution of equation (5) for Δu into equation (6) and integration yields

$$\frac{dL}{dy} = \frac{\rho U \Gamma}{\pi}\left(\tan^{-1}\frac{y_2 - y}{z} - \tan^{-1}\frac{y_1 - y}{z} + \tan^{-1}\frac{\frac{a^2}{y_1} - y}{z} - \tan^{-1}\frac{\frac{a^2}{y_2} - y}{z}\right)$$

$$= \rho U \Gamma \frac{2}{\pi} \tan^{-1} \frac{z(y_1 - y_2)}{a^2 + y_1 y_2 - y(y_1 + y_2)} \tag{7}$$

Equation (7) is the equation for the lateral distribution of lift induced on the cylinder. This can be written as

$$\frac{1}{q\frac{b}{2}} \frac{dL}{dy} = 2 \frac{c_l c^*}{\pi} \tan^{-1} \frac{z(y_1 - y_2)}{a^2 + y_1 y_2 - y(y_1 + y_2)} \tag{7a}$$

since

$$\Gamma = \frac{bU}{4} c_l c^*$$

Integrating to get the total lift induced on the cylinder yields

$$L = \int_{-a}^{a} \frac{dL}{dy} \, dy$$

$$= \rho U \Gamma \left(\frac{a^2}{y_1} - \frac{a^2}{y_2}\right)$$

$$= \rho U \Gamma \, \Delta y^{(i)} \tag{8}$$

[redacted]

Since the longitudinal distribution of Δu is symmetrical about the plane $x = 0$, the location of the bound leg of the horseshoe vortex, the longitudinal center of pressure of the induced lift must be on the same longitudinal ordinate as the bound leg.

Superposition of lift due to several vortices.- In the more general case of the wing-tip-tank combination, the wing is replaced by several horseshoe vortices of convenient width, bound legs centered on the quarter-chord line of the wing, or the actual center-of-pressure location of the section, if known. The tip tank is represented by an infinite cylinder containing images of the wing vortices. A typical representation is shown in figure 2.

The lift induced on the cylinder by the complete wing vortex-image system can be calculated by superposing the lifts due to each of the vortices and their images. The lift induced on a cylinder by a group of m horseshoe vortices representing a wing then is

$$L = \sum_{n=1}^{m} \rho U \Gamma_n \left(\frac{a^2}{y_n - s_n} - \frac{a^2}{y_n + s_n} \right) \tag{9}$$

where y_n is the center of the nth wing vortex, s_n is the semispan of that vortex, Γ_n is the strength of that vortex, a is the radius of the cylinder, and $\frac{a^2}{y_n - s_n} - \frac{a^2}{y_n + s_n}$ is $\Delta y_n^{(i)}$, the width of the image vortex. In terms of the wing parameters and the dimensionless spanwise loading coefficient $c_l c^*$, the equation for the lift-curve slope of the tank is

$$\left(C_{L_t} \right)_\alpha = \frac{A}{2b} \sum_{n=1}^{m} \left(c_l c^* \right)_n \left(\frac{a^2}{y_n - s_n} - \frac{a^2}{y_n + s_n} \right) \tag{9a}$$

where $c_l c^* = \frac{4\Gamma}{bU}$ and y_n is measured from the center of the tank.

The moment arm of the induced lift of each vortex-image system $\bar{x}$ is measured from the center of moments to the bound leg of that system, and the total pitching moment induced on the cylinder is

$$M = \sum_{n=1}^{m} \Delta L_n \bar{x}_n = \sum_{n=1}^{m} \rho U \Gamma_n \left(\frac{a^2}{y_n - s_n} - \frac{a^2}{y_n + s_n} \right) \bar{x}_n \tag{10}$$

[redacted]

and the moment coefficient is

$$\left(C_{M_t}\right)_\alpha = \frac{A}{2b}\sum_{n=1}^{m}\left(c_l c^*\right)_n\left(\frac{a^2}{y_n - s_n} - \frac{a^2}{y_n + s_n}\right)\bar{x}_n''' \qquad (10a)$$

(The moment coefficient may be made dimensionless with respect to any length; however, in this report, for convenience in comparing calculated and experimental data, the tip-tank maximum diameter is used.)

Correction for finite length of tank.- To the preceding calculation of the induced lift, an approximate correction for the finite length of the tip tank may be made by using the same correction as that employed in reference 1 for fuselages. The portion of the tank downstream from the wing may be considered an infinite cylinder in all cases; whereas the portion ahead of the wing may be treated as a body of the slenderness ratio of the tank forebody. The correction factor should be half that for an infinite cylinder (unity) added to half that for the forebody (σ). The correction factor η is

$$\eta = \frac{1}{2}(1 + \sigma)$$

where σ is the correction factor given in reference 1 for ellipsoids of revolution. The correction factor η is plotted as a function of slenderness ratio in figure 3. It can be seen that if this factor is neglected, the error is less than 5 percent for most practical tip-tank slenderness ratios.

Calculation of Body-Alone Lift and Moment

Body-alone lift.- The induced lift on the tip tank is independent of the angle of attack of the tank and is dependent only on the wing lift distribution. There is, however, a component of the total lift on the tip tank due to its angle of attack which is referred to as the body-alone lift. In calculating this component of the total lift, the effect of upwash of the wing on the angle of attack will be neglected because the body lift is small compared to the induced lift. Since the wing tends to make the flow parallel to the tip-tank axis in the region of the junction of the two, there is negligible body-alone lift on that section of the tank. Because of the tip-tank wake, the lift on the section downstream from the location of maximum tank diameter is small, and for practical purposes, negligible. Therefore, the concern is mainly with the body lift over the section of the tank ahead of the

wing. An additional component of lift due to viscous effects which varies with the square of the angle of attack is not considered, since the angles of attack are assumed to be small.

The body-alone lift is calculated simply from Munk's airship theory (ref. 2) and is expressed as

$$L_B = \frac{\pi}{2}\left(K_2 - K_1\right) q \, d_{LE}{}^2 \alpha \tag{11}$$

where $K_2 - K_1$ is given in reference 2 as a function of the slenderness ratio, and d_{LE} is the diameter of the body at the wing-tip leading edge.

Body-alone moment.- The pitching moment for a slender body of revolution at an angle of attack is given by reference 2 as

$$M = 2q\alpha V\left(K_2 - K_1\right) \tag{12}$$

where V denotes the volume of the body of revolution and M is taken about the centroid of the body. The body-alone moment of the tank will be

$$M = 2q\alpha V'\left(K_2 - K_1\right) \tag{12a}$$

where V' denotes the volume of the portion of the tank ahead of the wing-tip leading edge except when the maximum diameter of the tank occurs ahead of the wing-tip leading edge. In this case V' is the volume of the portion of the tank ahead of the tank maximum diameter. The moment reference axis is at the wing-tip leading edge except when the tank maximum diameter is used, in which case the reference axis is at the tank maximum diameter. This procedure is illustrated in the numerical example given in the appendix.

Total tank lift and moment.- The total tank lift is the sum of the induced and body-alone lifts, calculated from equations (9) and (11). The total tank moment is the sum of the induced-lift and body-alone-lift moments, calculated from equations (10) and (12). These sums can be added to the wing lift and moment to produce the total lift and moment on the wing–tip-tank combination.

Spanwise Wing Lift Distribution

Outline of method.- In a manner similar to that of reference 1, the spanwise wing lift distribution is calculated by equating the angle of downwash induced at the three-quarter-chord line expressed in terms of the vortex strength to the geometric angle of attack at the three-quarter-chord line at several points along the span. The resulting simultaneous equations are solved for the vortex strengths. The vortex-image system can be used to calculate the downwash at the three-quarter-chord line (although the boundary conditions on the cylinder are not satisfied everywhere), provided certain corrections are made in the downwash functions. The approximate downwash factors calculated herein should be sufficiently accurate for most practical purposes; however, more accurate values may be used when they become available.

Downwash in region near bound vortices.- It was pointed out that the boundary conditions on the cylinder of the horseshoe vortex-image system are satisfied exactly only infinitely far behind the wing, in the plane $z = 0$, and in the plane $x = 0$. The additional potential necessary to satisfy the boundary conditions everywhere else which contributed nothing to the tank lift and moment, does induce a downwash. In the region near the bound vortex, the downwash due the additional potential must be considered. As suggested in reference 1, the effect of the additional potential will be approximated by a correction to the downwash of the bound vortices which will be assumed to take into account the greater part of the effect of the additional potential on the downwash at the three-quarter-chord line. This correction is used in the illustrative example in the appendix; however, for wing–tip-tank configurations, the ratio of tip chord to tank radius is usually large $\left(\text{say } \frac{c_T}{r_t} \geq 4\right)$ so that the effect on the lift distribution will be found to be small and the correction may be neglected if the best accuracy is not required. If the correction factor is neglected, the tables of reference 3 can be used to obtain most of the downwash functions so that the time required for making the calculations will be reduced somewhat.

The correction to the downwash of the bound vortices is obtained by treating the flow induced by the bound vortices normal to the wing three-quarter-chord line as a two-dimensional uniform rectilinear flow past a circular cylinder. The downwash velocity due to the bound vortices w is increased then by $\left(\frac{r_t}{y_{ot} - y_p}\right)^2 w$ where $y_{ot} - y_p$ is the lateral distance from the center of the tank to the point on the wing at which the downwash is to be calculated.

[redacted]

Replacing the wing by m horseshoe vortices of convenient width, the expression for the downwash angle at any point $p(x,y)$ can be written

$$\left(\frac{w}{U}\right)_p = \sum_{n=1}^{m} \frac{\left(c_l c^*\right)_n}{\pi} \frac{b}{16} \left\{ F_{np} + G_{np} \left[1 + \left(\frac{r_t}{y_{ot} - y_p} \right)^2 \right] \right\} \tag{13}$$

where $\left(c_l c^*\right) = \dfrac{2\Gamma_n}{U \dfrac{b}{2}}$ and F_{np} is the downwash function of the trailing legs of vortex Γ_n located at x_n,y_n and its images on station x_p,y_p, and G_{np} is the downwash function of the bound leg of this vortex and its images on station x_p,y_p.

From the Biot-Savart law, F_{np} is the sum of terms having the form

$$F_{np} = \frac{1}{y_p - y_n \pm s_n} \left[1 + \frac{x_p - x_n}{\sqrt{\left(y_p - y_n \pm s_n\right)^2 + \left(x_p - x_n\right)^2}} \right] \tag{14}$$

and G_{np} is the sum of terms having the form

$$G_{np} = \frac{1}{x_p - x_n} \left| \frac{y_p - y_n + s_n}{\sqrt{\left(y_p - y_n + s_n\right)^2 + \left(x_p - x_n\right)^2}} - \frac{y_p - y_n - s_n}{\sqrt{\left(y_p - y_n - s_n\right)^2 + \left(x_p - x_n\right)^2}} \right| \tag{15}$$

where s_n is the semispan of the nth horseshoe vortex. If the correction to G_{np}, $\left(\dfrac{r_t}{y_{ot} - y_p}\right)^2$, is not used, the values $F_{np} + G_{np}$ can be obtained from the tables of reference 3.

[redacted]

The local angle of attack of the section must be corrected at p as in reference 1 for the presence of the cylinder in the free stream. The vertical component of the free stream w is affected by the cylinder in the same manner as the bound-leg flow; the correction factor (which may not be neglected) is again $\left(\frac{r_t}{y_{ot} - y_p}\right)^2$. Therefore

$$\alpha_{p_{eff}} = \alpha_{gp} + \left(\frac{r_t}{y_{ot} - y_p}\right)^2 \alpha_t \tag{16}$$

The final equation for downwash on the pth station on the wing of a wing–tip-tank combination is

$$\left(\frac{w}{U}\right)_p = \sum_{n=1}^{m} \frac{(c_l c^*)_n}{\pi} \frac{b}{16} \left\{ F_{np} + G_{np} \left[1 + \left(\frac{r_t}{y_{ot} - y_p}\right)^2 \right] \right\} = \alpha_{p_{eff}} \tag{17}$$

Now at all the downwash stations located midway between the trailing legs of the wing horseshoe vortices, an equation for the downwash can be written and equated to the effective angle of attack α_{eff}. The resulting m linear equations with m unknowns can be solved simultaneously for the values of $(c_l c^*)_n$.

It may be noted that the Prandtl-Glauert compressibility correction may be used if desired in calculating the loading on the wing at higher Mach numbers. Only the calculation of the spanwise lift distribution on the wing is changed in this case. All the other calculations described in this paper will be unaffected.

The values of $(c_l c^*)_n$ can be used immediately in equations (7a), (9a), and (10a) to get the lift distribution, total lift, and moment induced on the tip tank.

APPLICATION OF METHOD AND COMPARISON OF RESULTS WITH EXPERIMENT

Used in the application of the method of this report are the wing–tip-tank configurations of reference 4, for which experimental data on tank lifts and moments were available. These wing–tip-tank configurations are similar to those in general use: aspect ratio, 5.25; taper

ratio, 0.39; sweep, 12.7°; ratio of radius of tip tank to tip chord of wing, 0.25; slenderness ratios of tanks, 6:1 and 8:1. The comparison of the method with the experimental data for this case should indicate whether the method will be valid for most wing–tip-tank combinations.

In the numerical example in the appendix, the wing is replaced by several (that is, 10) horseshoe vortices of convenient width, and the tip tank by a system of images of the wing vortices, as shown in figure 2(b). Since the induced lift on the tip tank depends strongly on the lift distribution near the wing tip, smaller wing vortices were used at the tip to give better accuracy in that region. Using equation (17) for the downwash, the spanwise distribution of lift is determined for the wing, and then by equations (9), (10), (11) and (12), the lift and moment of the tip tank are calculated. It is to be noted that if the spanwise lift distribution on the wing in the presence of tip tanks is known, the computation is reduced by a considerable amount.

A comparison of experimental results with those obtained from the numerical example in the appendix is summarized as follows ($\bar{x}'''$ is positive forward of the tank center of gravity in the following tabulation):

		Theory	Experiment	Difference (based on experimental value)
$\left(C_{L_{wo}}\right)_\alpha$		4.32	4.06	6.4 percent
$\left(C_{L_{wt}}\right)_\alpha$		4.74	4.45	6.5 percent
$\dfrac{\left(C_{L_{wt}}\right)_\alpha - \left(C_{L_{wo}}\right)_\alpha}{\left(C_{L_{wo}}\right)_\alpha}$		0.097	0.096	1.0 percent
$\dfrac{\left(C_{L_t}\right)_\alpha}{\left(C_{L_{wo}}\right)_\alpha}$	Central	0.0185	0.0172	7.6 percent
	Forward	0.0192	0.0175	9.7 percent
	Rearward	0.0185	0.0174	6.3 percent
$\bar{x}''' = \dfrac{\left(C_{M_t}\right)_\alpha}{\left(C_{L_t}\right)_\alpha}$	Central	0.955	0.884	1.2 percent tank length
	Forward	0.289	0.623	4.1 percent tank length
	Rearward	2.000	2.140	1.8 percent tank length

Figures 4 to 6 show comparisons of experimental values of C_{L_t} and C_{M_t} with theoretical values plotted from values of $\left(C_{L_t}\right)_\alpha$ and

[redacted]

$\left(C_{M_t}\right)_\alpha$ determined by the method of this paper, assuming the zero lift points to be those indicated by experiment. Figures 7 and 8 present the calculated spanwise lift distributions over the wing, wing–tip-tank combination, and over the tip tank. The small difference between the calculated and experimental values of $\frac{\left(C_{L_{wt}}\right)_\alpha - \left(C_{L_{wo}}\right)_\alpha}{\left(C_{L_{wo}}\right)_\alpha}$ indicates that the method of calculating wing–tip-tank interference is good. The larger differences between calculated and experimental values of $\left(C_{L_{wo}}\right)_\alpha$ and $\left(C_{L_{wt}}\right)_\alpha$ can be attributed, in part at least, to the simplified representation of the wing by only ten vortices.

Since the induced lift on the tip tanks is a function of the spanwise circulation on the wing, the agreement between calculated and experimental values of tank lift indicates that the calculated spanwise wing lift distribution is valid, although the experimental distribution of lift over the wing–tip-tank combination was not available.

Since the body-alone lift and moment are only small parts of the total lift and moment on the tip tank in the presence of the wing, the approximations used in simplifying the calculations of the body-alone lift and moment are considered to be good enough for the purposes of the analysis in this paper. A possible exception will be the case of the extreme forward tank, where the body-alone lift is sufficiently far forward to produce an appreciable contribution to the tank pitching moment. More accurate methods of calculating the body-alone lift and moment might be employed to improve the accuracy of the calculation of the total tank lift and moment in the extreme forward case.

CONCLUSIONS

A method of analysis has been developed for calculating the loading on wing–tip-tank combinations in subsonic flow, taking into account wing–tip-tank interference. Good agreement with experimental results for the lift on the combination, the lift on the tip tank, and the center of pressure on the tip tank were obtained for three typical configurations. The error in the calculated center-of-pressure location on the tip tank for the case of a tank located with the nose far ahead of the wing-tip leading edge was found to be greater than the errors in the other calculated results. Since the loading on the tip tank depends largely on the spanwise lift distribution on the wing, the calculated

spanwise loading would also be expected to be in good agreement with spanwise lift distributions obtained by experiment, although the latter were not available for comparison.

Langley Aeronautical Laboratory,
National Advisory Committee for Aeronautics,
Langley Field, Va.

APPENDIX

NUMERICAL EXAMPLE

Geometry of Configuration

In order to illustrate the method, calculations will be made for the wing–tip-tank configurations used in the tests reported in reference 4. Experimental model dimensions are wing span, 92.08 inches and tank radius, 1.97 inches and the geometric characteristics as given in reference 4 are:

Aspect ratio	5.25
Taper ratio	0.393
Sweep (quarter chord), deg	12.7
Tip-tank radius, $\frac{r_t}{b/2}$	0.04275

Tank slenderness ratios, $\frac{e}{d_{max}}$

Central case	6.0
Rearward case	8.0
Forward case	8.0

Location of tank center of gravity, rearward of wing-tip leading edge, $\frac{x_{cg}}{d_{max}} = x_{cg}'''$

Central case	0.80
Rearward case (aft case of ref. 4)	1.81
Forward case	-0.195

The plan form of the wing is shown in figure 2(a) and the various tip-tank configurations in figure 2(c).

Calculation of Spanwise Lift Distribution on Wing

Coordinates of lift and downwash stations.- The wing will be represented by five horseshoe vortices on each semispan, three inboard vortices of span $\frac{1}{4}\frac{b}{2}$, and two outboard of span $\frac{1}{8}\frac{b}{2}$. The bound legs

are centered on the quarter-chord line and the downwash points are located on the three-quarter-chord line, midway between the trailing legs. The origin is at the intersection of the quarter-chord line with the axis of symmetry. All distances in this section will be made dimensionless with respect to s, the semispan of the inboard wing horseshoe vortices. The center of each bound leg will be called a "lift point." (See fig. 2(a).) The coordinates of the lift points are as follows:

n	$\pm y_n'$	x_n'
1	1.00	0.2254
2	3.00	.6761
3	5.00	1.1268
4	6.50	1.4648
5	7.50	1.6902

The coordinates of the downwash points are:

p	$\pm y_p'$	x_p'
1	1.00	2.2486
2	3.00	2.3670
3	5.00	2.4844
4	6.50	2.5739
5	7.50	2.6334

The coordinates of the image lift points are:

n	$\pm y_n'$	x_n'
5'	8.1275	1.6902
4'	8.2736	1.4648
3'	8.3038	1.1268
2'	8.3288	.6761

The case where $n = 2'$ denotes a single vortex which represents in addition to $\Gamma_2^{(i)}$ all the successively smaller images between $\Gamma_2^{(i)}$ and the center of the cylinder (see fig. 2(b)).

[redacted]

Calculation of downwash.- The downwash function for the trailing legs F_{np} is the sum of f_{np} (the downwash function of the vortex located at lift point x_n,y_n (on p)), f_{np}' (the downwash function of the vortex at lift point $x_n,-y_n$), and $f_{np}^{(i)}$ and $f_{np}^{(i)'}$ (the downwash functions for the trailing legs of the two image vortices (one in each tank))

$$F_{np} = f_{np} + f_{np}' + f_{np}^{(i)} + f_{np}^{(i)'}$$

and similarly for the bound legs

$$G_{np} = g_{np} + g_{np}' + g_{np}^{(i)} + g_{np}^{(i)'}$$

Making equations (14) and (15) dimensionless with respect to $s = \frac{b}{16}$ yields

$$f_{np} = \frac{1}{y_p' - y_n' + s_n'}\left[1 + \frac{x_p' - x_n'}{\sqrt{(x_p' - x_n')^2 + (y_p' - y_n' + s_n')^2}}\right] - \frac{1}{y_p' - y_n' - s_n'}\left[1 + \frac{x_p' - x_n'}{\sqrt{(x_p' - x_n')^2 + (y_p' - y_n' - s_n')^2}}\right] \tag{A1}$$

and

$$g_{np} = \frac{1}{x_p' - x_n'}\left|\frac{y_p' - y_n' + s_n'}{\sqrt{(y_p' - y_n' + s_n')^2 + (x_p' - x_n')^2}} - \frac{y_p' - y_n' - s_n'}{\sqrt{(y_p' - y_n' - s_n')^2 + (x_p' - x_n')^2}}\right| \tag{A2}$$

[redacted]

Since the loading is symmetrical $\left(\Gamma(x_n,y_n) = \Gamma(x_n,-y_n)\right)$, only the downwash on one half of the wing need be computed. In order to calculate the downwash function on station 5 due to all vortices of strength Γ_5, substitute the values of x_n' and y_n' for $n = 5$, and x_p' and y_p' for $p = 5$ $\left(s_n'\right.$ in this case is equal to $0.5\left.\right)$ in equations (A1) and (A2); then

$$f_{5,5} = \frac{1}{0.5}\left[1 + \frac{2.6334 - 1.6902}{\sqrt{(2.6334 - 1.6902)^2 + (0.5)^2}}\right] -$$

$$\frac{1}{-0.5}\left[1 + \frac{2.6334 - 1.6902}{\sqrt{(2.6334 - 1.6902)^2 + (0.5)^2}}\right]$$

$$f_{5,5} = 7.5342$$

Similarly,

$$g_{5,5} = 0.9932$$

$$f_{5,5}' = -0.0050$$

$$g_{5,5}' = 0.0003$$

$$f_{5,5}^{(i)} = -1.4084$$

$$g_{5,5}^{(i)} = 0.1660$$

and the functions $f_{5,5}^{(i)'}$ and $g_{5,5}^{(i)'}$ of the opposite image are negligible.

The correction factor for the bound-leg downwash function $1 + \left(\frac{r_t}{y_{ot} - y_p}\right)^2$ at station $p = 5$ is

[redacted]

$$1 + \left(\frac{0.3420}{0.8421}\right)^2 = 1.1652$$

so

$$F_{5,5} = \sum f_{5,5} = 6.1208$$

and

$$G_{5,5} = \sum g_{5,5} = 1.1595$$

and the total downwash function is

$$F_{5,5} + \left[1 + \left(\frac{r_t}{y_{ot} - y_p}\right)^2\right] G_{5,5} = 7.47361$$

The calculation of $F_{4,5}$, $G_{4,5}$, $F_{3,5}$, $G_{3,5}$, $F_{2,5}$, and $G_{2,5}$ is similar. $F_{1,5}$ and $G_{1,5}$ do not include downwash functions due to images of Γ_1, because these are included as parts of the total image represented by $\Gamma_2^{(i)}$. Care must be taken that the proper value of s_n be substituted in computing f_{np} and g_{np}.

Distribution of lift over wing.- The downwash at point 5 can now be written

$$\left(\frac{W}{U}\right)_5 = \frac{1}{\pi}\Big[-0.10021\left(c_l c^*\right)_1 - 0.23465\left(c_l c^*\right)_2 - 0.67227\left(c_l c^*\right)_3 - 2.50802\left(c_l c^*\right)_4 + 7.47361\left(c_l c^*\right)_5\Big]$$

and a similar treatment of the other four downwash points gives the set of simultaneous equations for $\left(\frac{W}{U}\right)_p$ in $\left(c_l c^*\right)_n$. These are as follows:

[redacted]

$$\left.\begin{aligned}
\left(\frac{W}{U}\right)_1 &= 3.03506\Gamma_1^* - 1.31827\Gamma_2^* - 0.24018\Gamma_3^* - \\
&\quad 0.04918\Gamma_4^* - 0.04458\Gamma_5^* \\
\left(\frac{W}{U}\right)_2 &= -1.48562\Gamma_1^* + 4.24930\Gamma_2^* - 1.11661\Gamma_3^* - \\
&\quad 0.12065\Gamma_4^* - 0.08244\Gamma_5^* \\
\left(\frac{W}{U}\right)_3 &= -0.21090\Gamma_1^* - 1.20623\Gamma_2^* + 4.45794\Gamma_3^* - \\
&\quad 0.81303\Gamma_4^* - 0.25910\Gamma_5^* \\
\left(\frac{W}{U}\right)_4 &= -0.14247\Gamma_1^* - 0.30619\Gamma_2^* - 2.75001\Gamma_3^* + \\
&\quad 8.38920\Gamma_4^* - 2.43846\Gamma_5^* \\
\left(\frac{W}{U}\right)_5 &= -0.10021\Gamma_1^* - 0.23465\Gamma_2^* - 0.67227\Gamma_3^* - \\
&\quad 2.50802\Gamma_4^* + 7.47361\Gamma_5^*
\end{aligned}\right\} \qquad (A3)$$

where

$$\Gamma_n^* = \frac{\left(c_l c^*\right)_n}{\pi}$$

Now the geometric angle of attack, corrected to its effective value in the presence of the cylindrical tank by equation (16), is, since the wing is untwisted and the tank is not at an angle of incidence $(\alpha_t = \alpha_g)$,

$$\alpha_1 = 1.00210$$

$$\alpha_2 = 1.00397$$

$$\alpha_3 = 1.01496$$

[redacted]

$$\alpha_4 = 1.03452$$

$$\alpha_5 = 1.16516$$

for a unit geometric angle of attack. Equating the effective angle of attack to the downwash angle in equations (A3) and solving for $(c_l c^*)_n$ yields the spanwise lift distribution over the wing

$$(c_l c^*)_1 = 2.06175$$

$$(c_l c^*)_2 = 1.96321$$

$$(c_l c^*)_3 = 1.66579$$

$$(c_l c^*)_4 = 1.38555$$

$$(c_l c^*)_5 = 1.18883$$

These values are plotted in figure 7. The lift-curve slope of the wing in the presence of the tip tank is

$$\left(\frac{L}{qS}\right)_\alpha = (C_L)_\alpha = \frac{A}{2}\sum_{n=1}^{5}(c_l c^*)_n(\Delta y^*)_n = 4.58$$

Calculation of Induced Lift on Tip Tanks

Induced lift.- When the wing lift distribution in the presence of the tip tank is known and represented by a set of finite-width horseshoe vortices, the lift induced on an attached cylindrical body at the tip is, by equation (9a),

$$(C_{L_t})_\alpha = \sum \frac{A}{4}(c_l c^*)_n\left(\Delta y^{*(i)}\right)_n$$

where $\left(\Delta y^{*(i)}\right)_n$ is the width of the image of the nth wing vortex. Substituting $(c_l c^*)_n$ and $\left(\Delta y^{*(i)}\right)_n$ yields

[redacted]

$$\left(C_{L_t}\right)_\alpha = 1.3125\Big[(1.188)(0.03185) + (1.386)(0.00465) + (1.666)(0.00288) + (1.963)(0.00337)\Big]$$

$$= 0.07318$$

for one cylindrical tip tank. The correction factor for the finite length of the tank for a nose-section slenderness ratio of 5.4:1 is 0.945 from figure 3, so that the total induced lift coefficient on one tip tank for the central and rearward configurations is

$$\left(C_{L_t}\right)_\alpha = (0.945)(0.07318) = 0.0692$$

For the tank in the forward position the correction is 0.955 for the assumed slenderness ratio of 7.5:1 and

$$\left(C_{L_t}\right)_\alpha = (0.955)(0.07318) = 0.0699$$

Lateral distribution of induced lift.- Equation (7) which gives the lateral distribution of induced lift on the tank due to a single horseshoe vortex and its image can be written

$$\left(\frac{\Delta \frac{dL_t}{dy}}{q\,\frac{b}{2}}\right)_\alpha = \frac{2}{\pi}\left(c_l c^*\right)_n \tan^{-1} \frac{2s_n''\sqrt{1 - y^{2''}}}{1 + \left(y_n'' + s_n''\right)\left(y_n'' - s_n''\right) - 2y_n''y''}$$

where the double prime '' denotes dimensionless with respect to r_t, the radius of the tip tank, s_n'' is the semispan of the nth horseshoe vortex and y_n'' is the distance from the center of the tank to the lift point of the nth vortex. The section lift at a station y'' on the tank then is

[redacted]

$$\left(\frac{\frac{dL_t}{dy}}{q\frac{b}{2}}\right)_\alpha = \frac{2}{\pi}\sum_n \left(c_l c^*\right)_n \tan^{-1}\frac{2s_n''\sqrt{1-y^{2''}}}{1+\left(y_n''+s_n''\right)\left(y_n''-s_n''\right)-2y_n''y''}$$

$$\equiv \frac{2}{\pi}\sum_n \left(c_l c^*\right)_n \theta_n$$

The values of $\left(\frac{\Delta\frac{dL_t}{dy}}{q\frac{b}{2}}\right)_\alpha$ at $y'' = 0.5$ are calculated in the following table:

n	tan θ_n	θ_n/π	$\left(c_l c^*\right)_n\left(\theta_n/\pi\right)2 = \left(\frac{\Delta\frac{dL_t}{dy}}{q\frac{b}{2}}\right)_\alpha$
5	1.029	0.2545	0.6050
4	.1180	.0375	.1038
3	.0648	.0206	.0686
2	.0217	.0069	.0271
1	.01205	.00384	.0158
-1	.00708	.0023	.0093

For $y'' = 0.5$

$$\frac{1}{q\frac{b}{2}}\left(\frac{dL_t}{dy}\right)_\alpha = \sum_n \frac{2}{\pi}\left(c_l c^*\right)_n \theta_n = 0.83$$

[redacted]

The lifts at some other stations, which have been calculated similarly, are tabulated below and are plotted in figure 8.

y''	$\frac{dL/dy}{q\ b/2}$
.9	1.0385
.5	.8296
0	.6270
-.5	.4195
-.9	.1763
-1.0	.0000

Calculation of body-alone lift.- In the cases of the central and rearward tip-tank configurations, the slenderness ratio of the tank section ahead of the wing-tip leading edge is 3.92:1, $K_2 - K_1$ is 0.778, and $\frac{d_{LE}}{b/2}$ is $\frac{3.86}{46.04}$. From equation (11), the body-alone lift is

$$L_B = q\alpha \frac{\pi}{2} d_{LE}^2 (K_2 - K_1)$$

and

$$\left(C_{L_B}\right)_\alpha = \frac{L_B}{qS}$$

$$= \frac{\pi}{2} \frac{A}{4} \left(\frac{d_{LE}}{b/2}\right)^2 (K_2 - K_1)$$

$$= \frac{\pi}{8}(5.25)\left(\frac{3.86}{46.04}\right)^2 (0.778)$$

$$= 0.01124$$

[redacted]

For the forward tip-tank configuration, the slenderness ratio of the nose section is 5.4:1 so that $K_2 - K_1$ is 0.873, and $\frac{d_{LE}}{b/2} = \frac{3.94}{46.04}$

$$\left(C_{L_B}\right)_\alpha = \frac{\pi}{8}(5.25)\left(\frac{3.94}{46.04}\right)^2(0.873) = 0.01318$$

Total lift on tip tank.- The total coefficient of lift on the tip tank is the sum of the induced and body-alone lift coefficients, which in the central and rearward cases is

$$\left(C_{L_t}\right)_\alpha = 0.0692 + 0.0112 = 0.0804$$

and in the forward tank case is

$$\left(C_{L_t}\right)_\alpha = 0.0699 + 0.0132 = 0.0831$$

The values of C_{L_t} are plotted against $C_{L_{wo}}$ in figures 4(a), 5(a), and 6(a) for comparison with experiment.

Total Lift on Configuration

Wing-alone lift.- For comparison with the experimental data, the vortex representation of the wing shown in figure 2(a) was used in calculating the loading on the wing alone. The section lift coefficients so obtained are

n	$(c_l c^*)_n$
1	2.0196
2	1.9093
3	1.5850
4	1.2427
5	.8996

[redacted]

and the total wing-alone lift coefficient is

$$\left(C_{L_{wo}}\right)_{\alpha} = 2 \sum_{n=1}^{5} \frac{A}{4}\left(c_l c^*\right)_n \Delta y_n^* = 4.32$$

Wing-tip-tank combination lift.- The total lift coefficient of the wing-tip-tank combination is, for the central and rearward cases,

$$\left(C_{L_{wt}}\right)_{\alpha} = 4.5791 + 2(0.0804) = 4.74$$

so that the total increase in lift on the configuration due to adding tip tanks is

$$\Delta\left(C_L\right)_{\alpha} = 0.42$$

Calculation of Moments on Tip Tank

Moment of induced lift - (central tank).- The moment of the induced lift on the tip tank is the sum of the moments of all components of the induced lift. The center of pressure of each component is located at the same longitudinal station as the corresponding wing section center of pressure. These center-of-pressure locations were estimated using the curves of reference 5. The distance of each center of pressure from the wing-tip leading edge (dimensionless with respect to the tank diameter) is ($\bar{x}'''$ is positive rearward from the wing-tip leading edge)

n	$\bar{x}_m'''$
5	+0.27
4	-.09
3	-.44
2	-1.09

[redacted]

The moments of the individual components about the wing-tip leading edge are

n	$(c_l c^*)_n$	$(\Delta y^{*(i)})_n$	$\bar{x}_n''$	$c_l c^* (\Delta y^{*(i)})_n \bar{x}_n'''$
5	(1.188)	(0.0318)	(+0.27)	+0.0102
4	(1.386)	(.0047)	(-.09)	-.0006
3	(1.666)	(.0029)	(-.44)	-.0021
2	(1.963)	(.0034)	(-1.09)	-.0073

From equation 10(a),

$$\left(C_{M_t}\right)_\alpha = \frac{A}{4} \sum_n c_l c^* \left(\Delta y^{*(i)}\right)_n \bar{x}'''$$

so that about the wing-tip leading edge

$$\left(C_{M_t}\right)_\alpha = 0.0003$$

The coefficient of induced lift on the tank is $\left(C_{L_{t_i}}\right)_\alpha = 0.0692$. The center of pressure of induced lift (rearward of wing leading edge) on the tank therefore is

$$\bar{x}_t''' = \frac{0.0003}{0.0692} = 0.004$$

The moment coefficient of the induced lift about the tank center of gravity in the central case is

$$\left(C_{M_t}\right)_\alpha = (0.0692)(0.800 - 0.004) = 0.055$$

and in the rearward case

$$\left(C_{M_t}\right)_\alpha = 0.0692(1.810 - 0.004) = 0.125$$

[redacted]

In the forward case it is

$$\left(C_{M_t}\right)_\alpha = 0.0699(-0.19 - 0.004) = -0.014$$

Body-alone moment.- For the central and rearward cases the value of V' in equation 12(a) is equal to the volume of the portion of the tank which extends ahead of the wing leading edge. From the dimensions given in reference 4 for these two cases, this volume is half that of an ellipsoid of revolution having a slenderness ratio of 3.92:1 and a maximum diameter of 3.86 inches. (Note that in the coefficient C_{M_t} the reference length is still the actual value of $d_{max} = 3.94$ inches.) From reference 2 the value of $K_2 - K_1$ is 0.778. Then

$$\left(C_{M_{t_B}}\right)_\alpha = 2\frac{(V')}{S\,d_{max}}\left(K_2 - K_1\right)$$

$$= 2\frac{\frac{2\pi}{3}\frac{3.86}{2}^2(3.86)(3.92)}{(11.22)(144)(3.94)}(0.778)$$

$$= 0.0145$$

This moment is about the wing-tip leading edge, and to calculate it about the tank center of gravity, the center of pressure of the body lift must be known. The center of pressure (ahead of the leading edge) is

$$\bar{x}''' = \frac{\left(C_{M_{t_B}}\right)_\alpha}{\left(C_{L_{t_B}}\right)_\alpha} = \frac{0.0145}{0.0112} = 1.29$$

About the tank center of gravity, therefore, on the central tank

$$\left(C_{M_{t_B}}\right)_\alpha = 0.0112(1.29 + 0.80) = 0.023$$

[redacted]

and on the rearward tank

$$\left(C_{M_{t_B}}\right)_\alpha = 0.0112(1.29 + 1.81) = 0.035$$

For the forward case the V' in equation 12(a) is the volume of the portion of the tank ahead of the tank maximum diameter. From the dimensions in reference 4, the tank maximum diameter is located at $1.27\ d_{max}$ ahead of the wing-tip leading edge (or $1.07\ d_{max}$ ahead of the tank c.g.), and the shape of the tank ahead of the maximum diameter is that of an ellipsoid of revolution with a slenderness ratio of 5.4:1. The value of $K_2 - K_1$ in this case is 0.873. Then

$$\left(C_{M_{t_B}}\right)_\alpha = 2\,\frac{\frac{2\pi}{3}\left(\frac{3.94}{2}\right)^2\frac{(3.94)(5.4)}{2}}{(11.22)(144)(3.94)}(0.873)$$

$$= 0.0238$$

The center of pressure of the body lift is $1.80\ d_{max}$ ahead of the tank maximum diameter since $\bar{x}''' = \dfrac{\left(C_{M_{t_B}}\right)_\alpha}{\left(C_{L_{t_B}}\right)_\alpha} = 1.80$. The pitching-moment coefficient about the tank center of gravity is then

$$\left(C_{M_{t_B}}\right)_\alpha = \left(C_{L_{t_B}}\right)_\alpha (1.80 + 1.07)$$

$$= (0.01318)(1.80 + 1.07) = 0.038$$

Total tank moment.- The pitching-moment coefficient about the tank center of gravity in the central case is $\left(C_{M_t}\right)_\alpha = 0.055 + 0.023 = 0.078$, in the rearward case is $\left(C_{M_t}\right)_\alpha = 0.125 + 0.035 = 0.160$, and in the forward case is $\left(C_{M_t}\right)_\alpha = -0.014 + 0.038 = 0.024$. The values of C_{M_t} are plotted against $C_{L_{wo}}$ in figures 4(b), 5(b), and 6(b) for comparison with experiment.

[redacted]

REFERENCES

1. Zlotnick, Martin, and Robinson, Samuel W., Jr.: A Simplified Mathematical Model for Calculating Aerodynamic Loading and Downwash for Midwing Wing-Fuselage Combinations With Wings of Arbitrary Plan Form. NACA RM L52J27a, 1953.

2. Munk, Max M.: The Aerodynamic Forces on Airship Hulls. NACA Rep. 184, 1924.

3. Diederich, Franklin W.: Charts and Tables for Use in Calculations of Downwash of Wings of Arbitrary Plan Form. NACA TN 2353, 1951.

4. Fail, R., and Holford, J. F.: Preliminary Note on Low Speed Tunnel Model Tests of Pressure Distribution, Jettisoning and Drag of Tip Tanks on an Unswept Wing. TN No. Aero. 2085, British R.A.E., Nov. 1950.

5. Diederich, Franklin W.: A Simple Approximate Method for Calculating Spanwise Lift Distributions and Aerodynamic Influence Coefficients at Subsonic Speeds. NACA TN 2751, 1952.

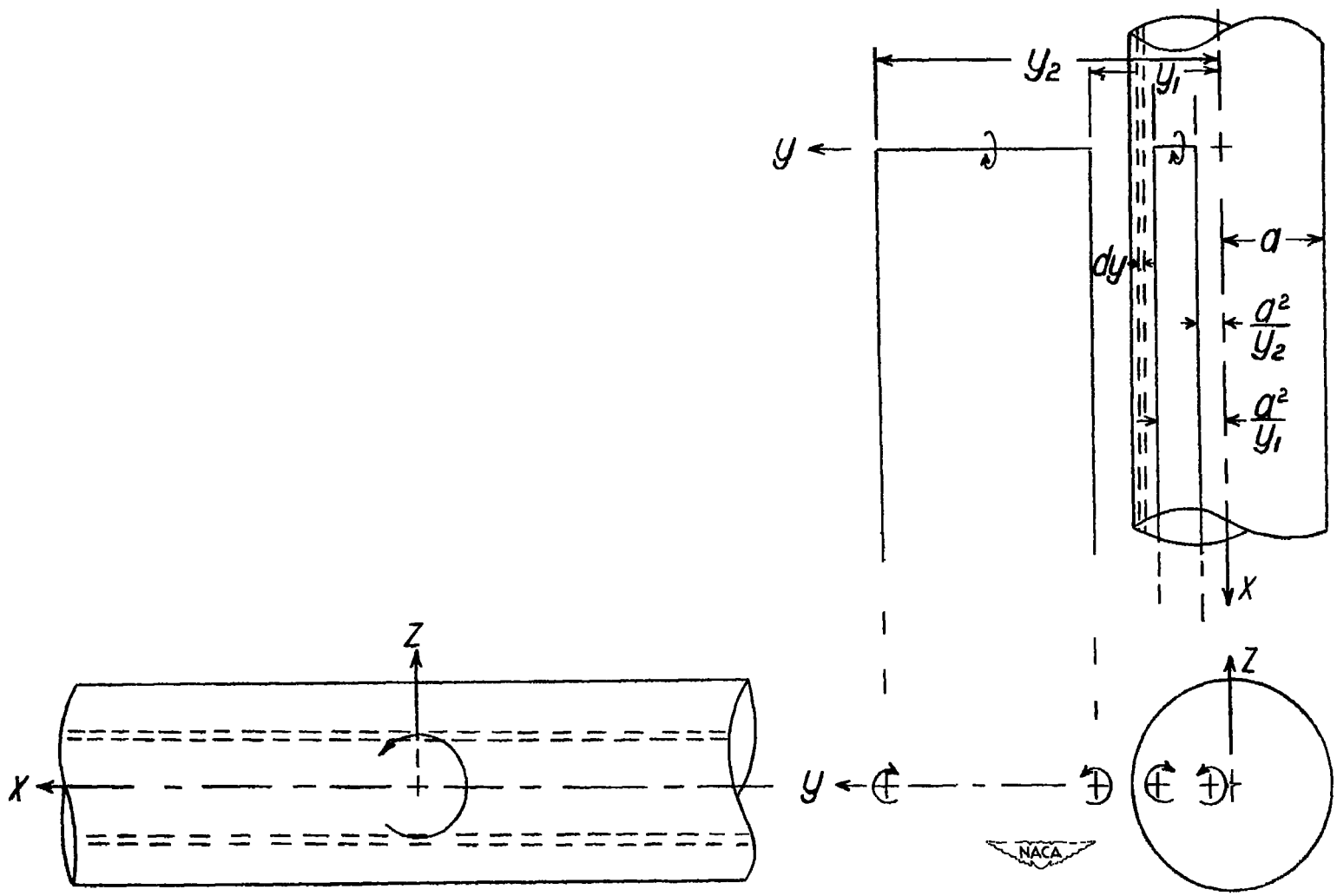

Figure 1.- Diagram of the horseshoe-vortex—infinite-cylinder combination with the image vortices within the cylinder.

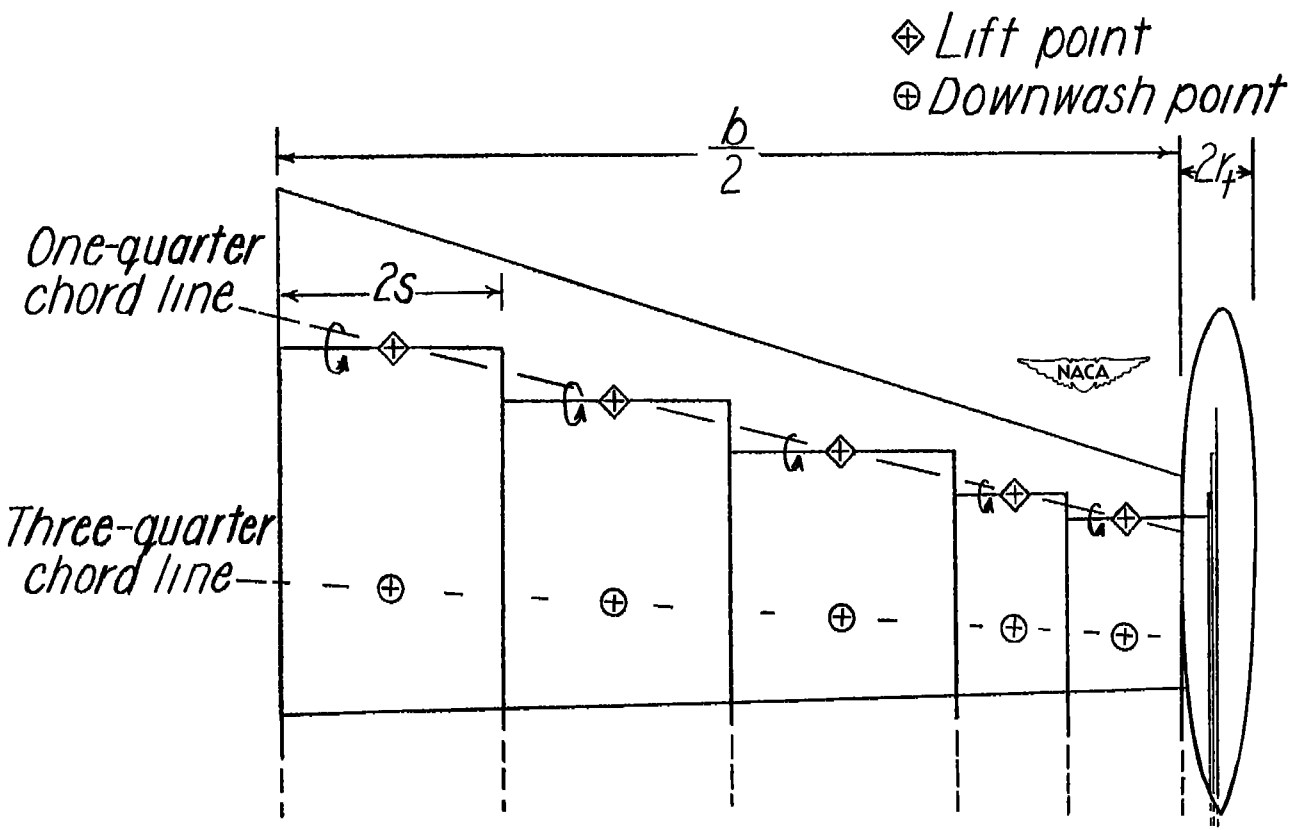

(a) Diagram of complete vortex-image system for the wing—tip-tank combination.

Figure 2.- Illustration of wing—tip-tank configuration and vortex-image system used in illustrative example.

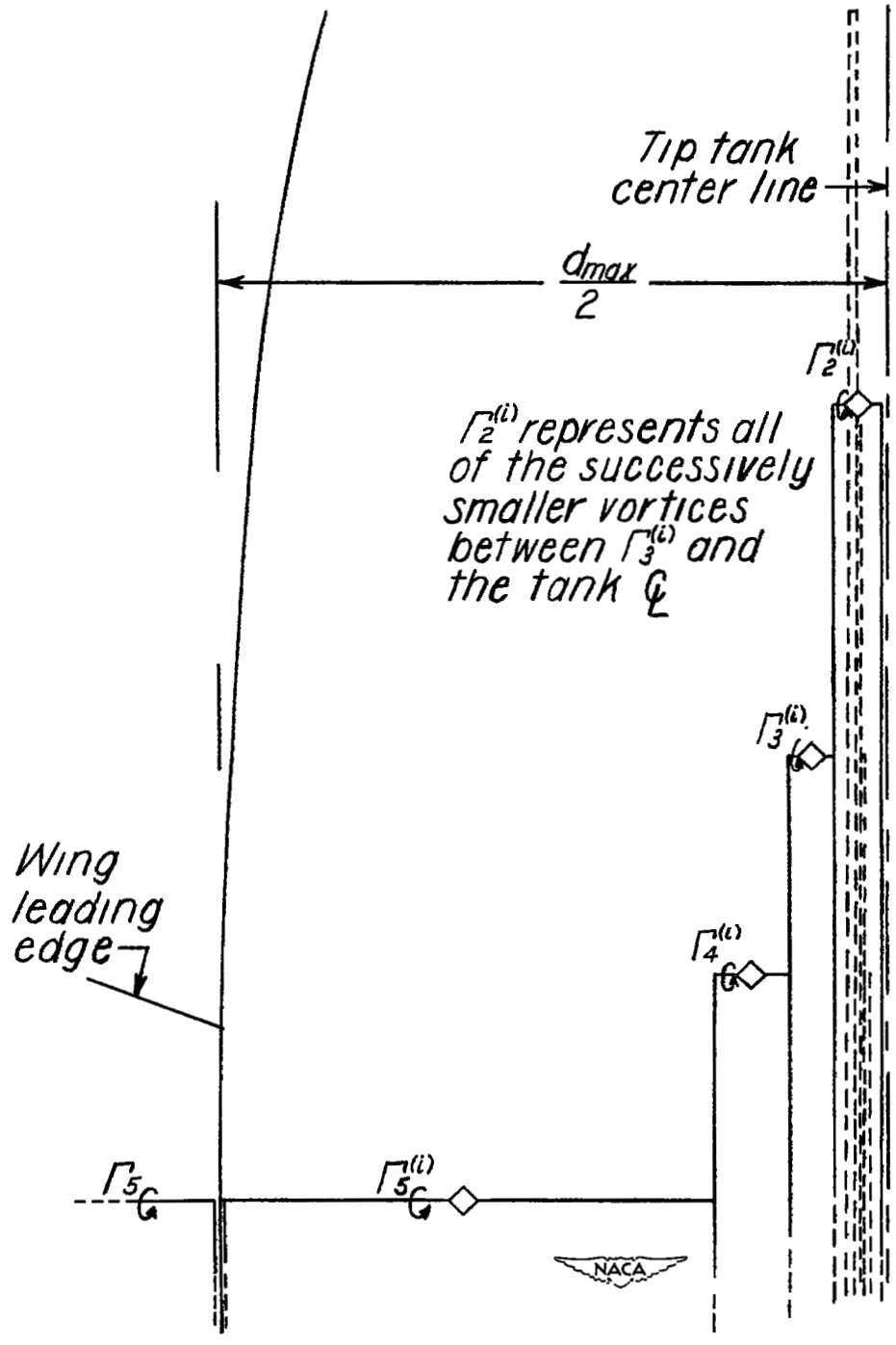

(b) Detailed diagram of the tip-tank image system.

Figure 2.- Continued.

[redacted]

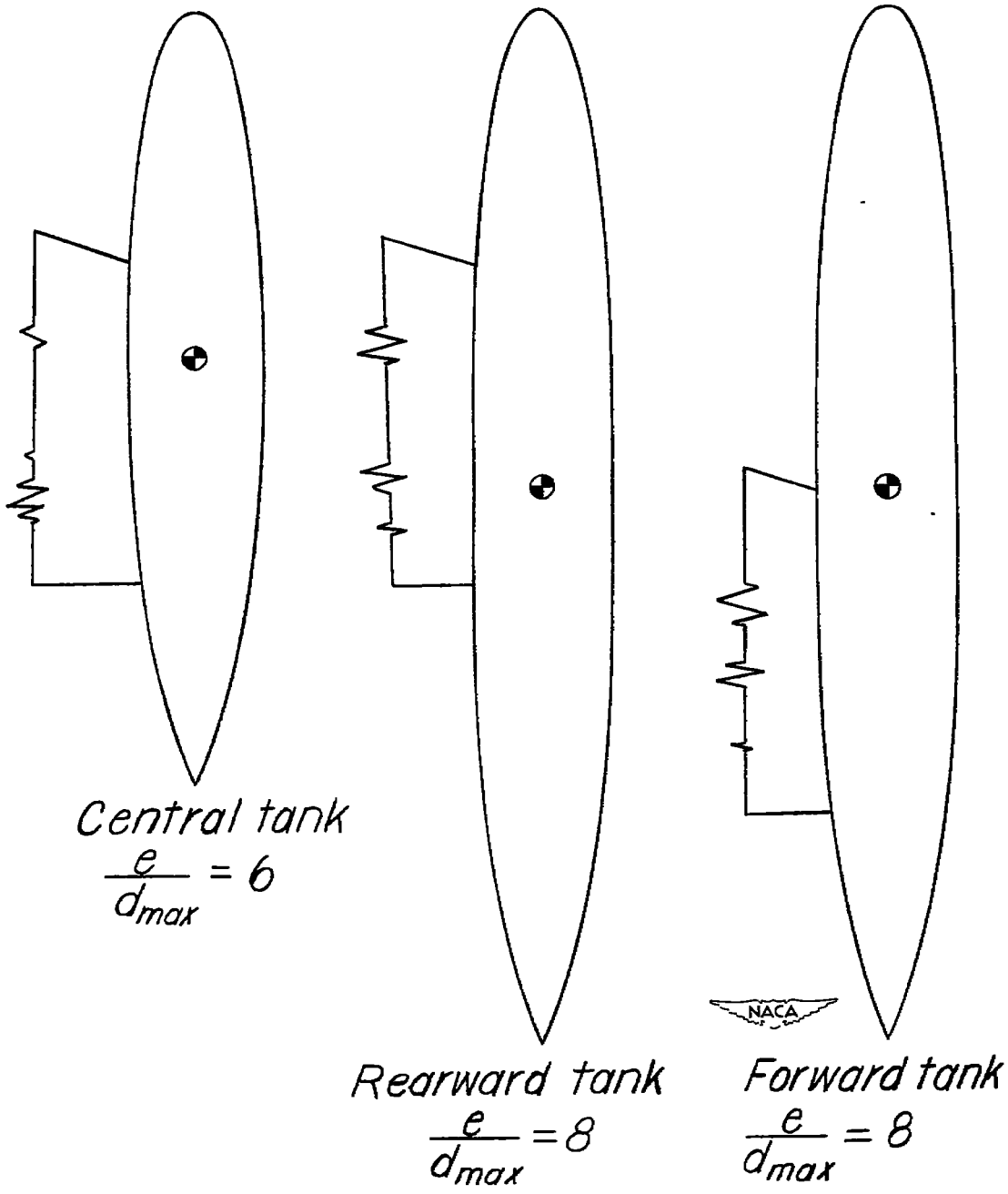

(c) Illustration of the three tip-tank locations considered.

Figure 2.- Concluded.

[redacted]

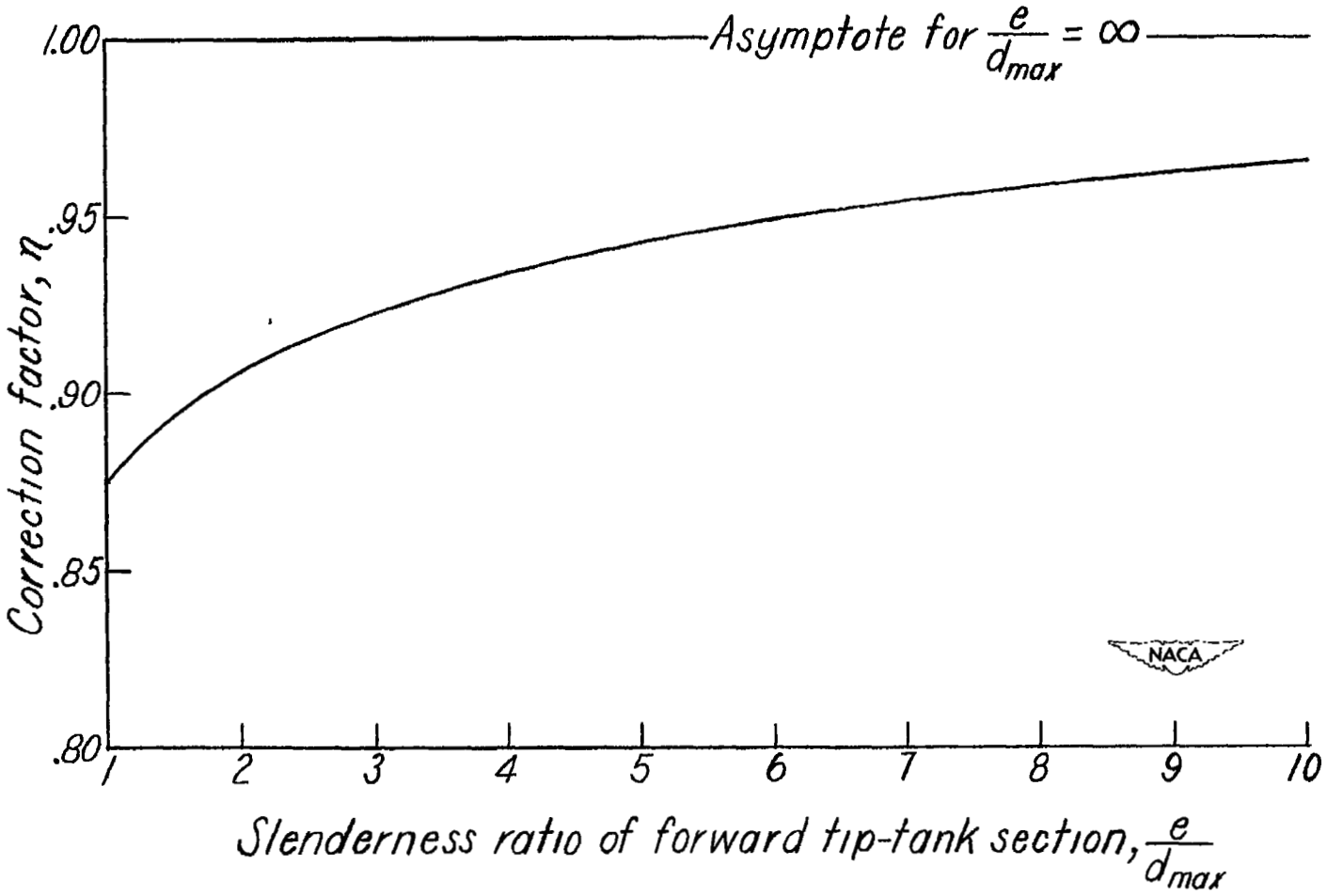

Figure 3.- Correction factor for the induced lift on the tip tank.

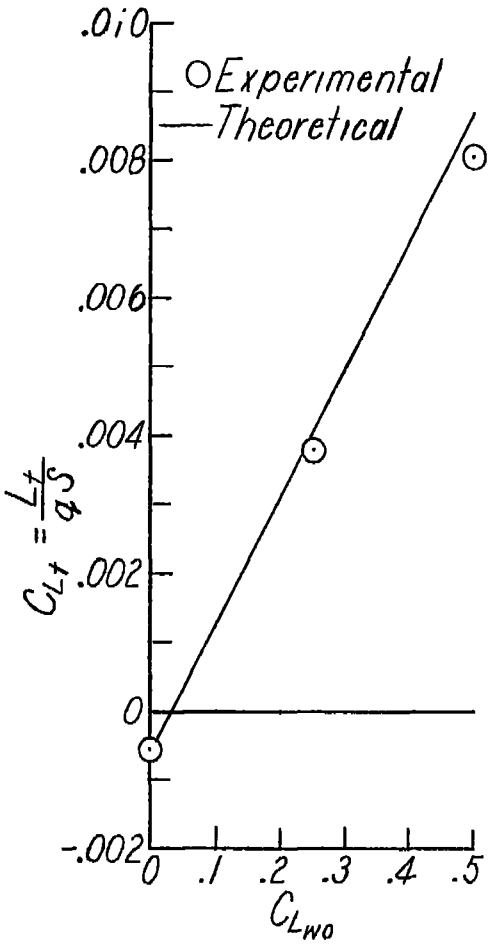

(a) Tip-tank lift coefficient.

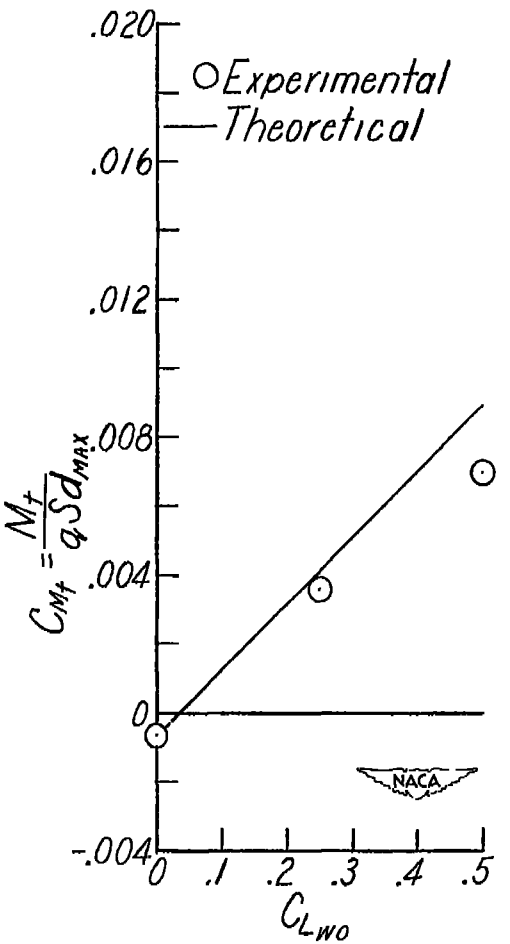

(b) Tip-tank pitching-moment coefficient.

Figure 4.- Comparison of theoretical and experimental tip-tank lift and pitching-moment characteristics. Central tank.

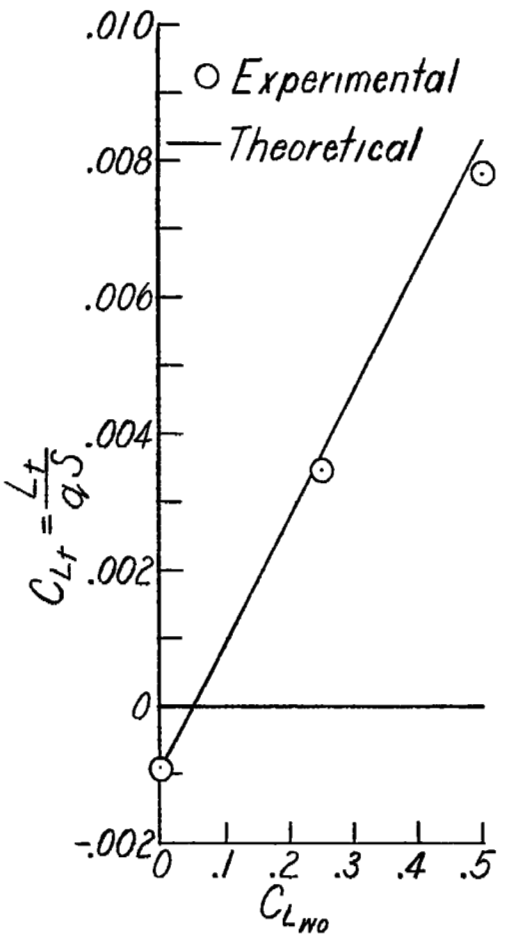

(a) Tip-tank lift coefficient.

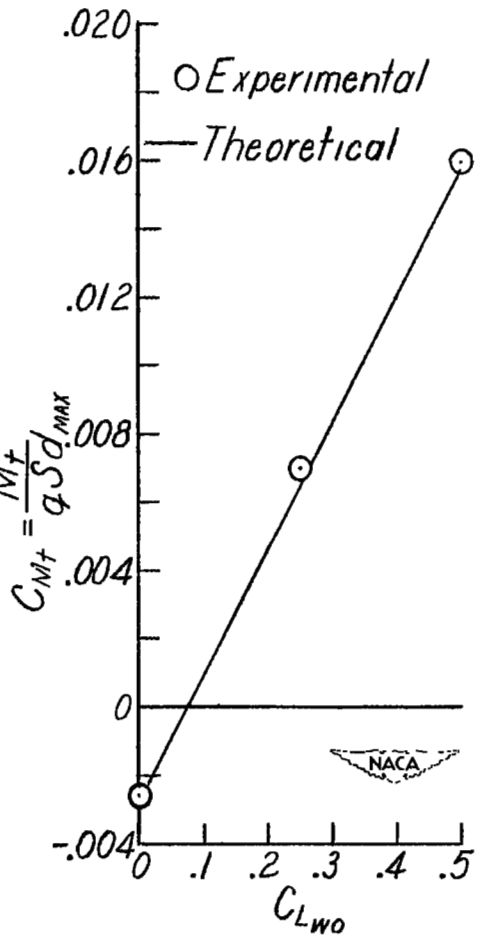

(b) Tip-tank pitching-moment coefficient.

Figure 5.- Comparison of theoretical and experimental tip-tank lift and pitching-moment characteristics. Rearward tank.

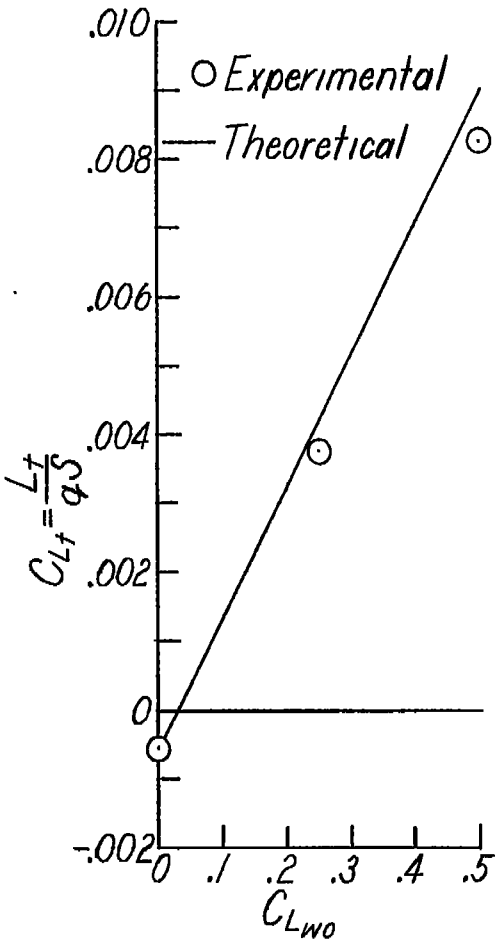

(a) Tip-tank lift coefficient.

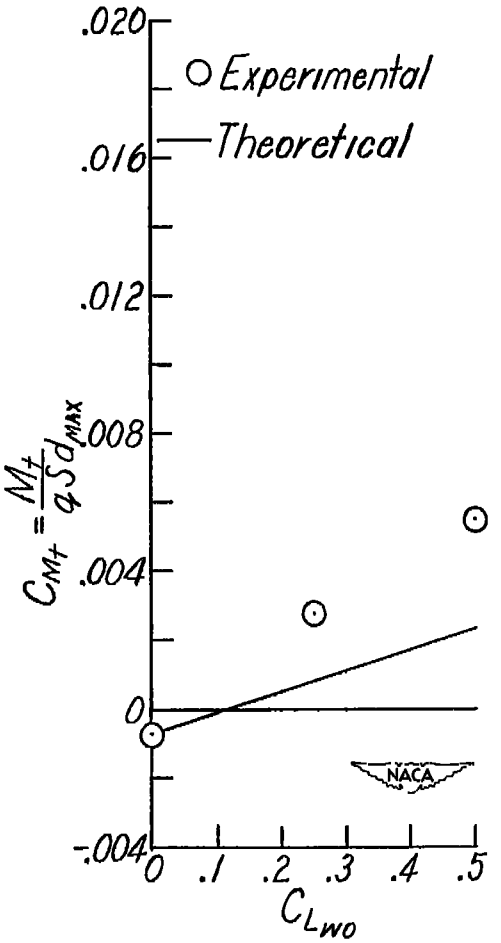

(b) Tip-tank pitching-moment coefficient.

Figure 6.- Comparison of theoretical and experimental tip-tank lift and pitching-moment characteristics. Forward tank.

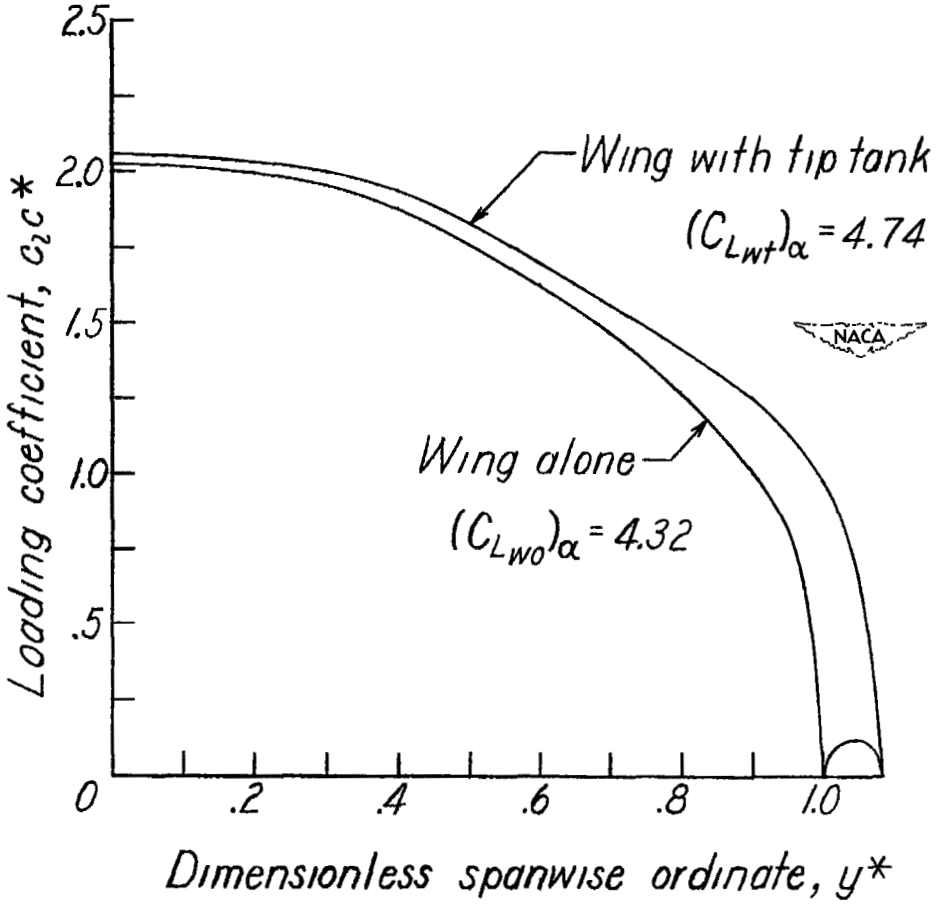

Figure 7.- Calculated spanwise lift distributions for a wing with and without tip tanks. $A = 5.25$; $\Lambda = 12.7^\circ$; $\lambda = 0.255$; $r_t^* = 0.0428$.

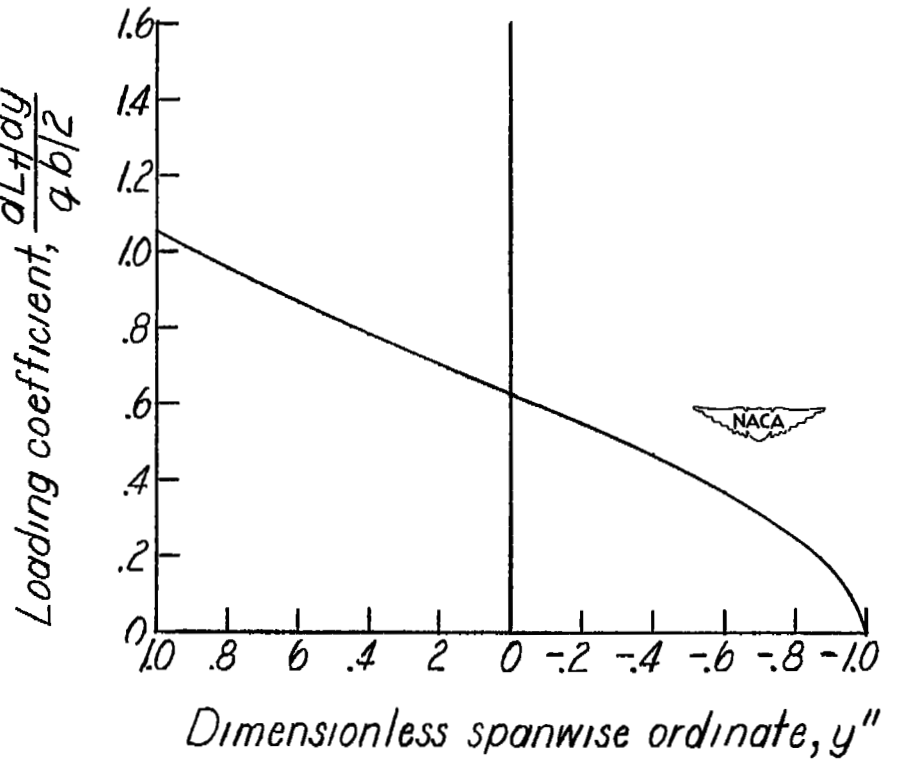

Figure 8.- Lateral distribution of induced lift over the tip tank.